

Low-temperature Reflection Spectra of the Single Crystals of TCNQ Complex Salts

Kyuya YAKUSHI, Masaaki IGUCHI, Gen KATAGIRI, Takahisa KUSAKA,
Toshiaki OHTA, and Haruo KURODA*

Department of Chemistry, Faculty of Science, The University of Tokyo, Hongo, Bunkyo-ku, Tokyo 113

(Received April 23, 1980)

The visible and near-infrared reflection spectra were measured, at temperatures in the range of 27–300 K, on the single crystals of (*N*-ethyl-1,10-phenanthroline)(TCNQ)₂, (methyltriphenylphosphonium)(TCNQ)₂ and Cs₂(TCNQ)₃. We found that the dispersion observed at about $(10\text{--}11) \times 10^3 \text{ cm}^{-1}$ in the reflection spectra of the former two salts is due to the local excitation associated with the lowest $\pi\text{--}\pi^*$ transition of (TCNQ)^{•−}. A new dispersion attributable to intermolecular charge transfer was found to appear at $(7\text{--}8) \times 10^3 \text{ cm}^{-1}$ in the spectrum of (methyltriphenylphosphonium)(TCNQ)₂ at low temperature. In the case of Cs₂(TCNQ)₃, the low-temperature spectrum showed that there are two dispersions in the range of $(8\text{--}14) \times 10^3 \text{ cm}^{-1}$, one of which being attributable to the charge transfer between (TCNQ)^{•−} ions and the other to the local excitation associated with (TCNQ)^{•−}. We propose a new interpretation for the spectra of TCNQ complex salts on the basis of these new experimental data.

The electronic spectra of TCNQ complex salts at room temperature have been studied by several authors.^{1–7)} The results of these investigations indicated that their spectra in the wave number region below $40 \times 10^3 \text{ cm}^{-1}$ are very similar to each other, commonly showing the following four strong absorption bands; the first one is at $(2\text{--}3) \times 10^3 \text{ cm}^{-1}$, the second at about $10 \times 10^3 \text{ cm}^{-1}$, the third at about $17 \times 10^3 \text{ cm}^{-1}$ and the fourth at about $30 \times 10^3 \text{ cm}^{-1}$, which we will denote as A, B, C, and D, respectively. Torrance *et al.* attempted to interpret the absorption spectra of TCNQ complex salts by comparing them with the absorption spectra of K(TCMQ) and Cs₂(TCNQ)₃.⁶⁾ They assigned the band A to the charge-transfer (CT) transition of the type (TCNQ)^{•−}-(TCNQ)⁰→(TCNQ)⁰(TCNQ)^{•−}, the band B to the CT transition of the type (TCNQ)^{•−}-(TCNQ)^{•−}→(TCNQ)⁰(TCNQ)^{2•−}, the band C to the local excitation (LE) associated with the lowest intramolecular transition of (TCNQ)^{•−}, and the band D to the LE associated with the lowest intramolecular transition of (TCNQ)⁰.

However, it should be noted that the band B is polarized in the direction appreciably different from the direction of TCNQ stack, and often exhibits a relatively sharp structure which resembles the vibrational structure of the lowest $\pi\text{--}\pi^*$ absorption band of (TCNQ)^{•−} ion in the solution. This is rather unusual for an absorption band associated with a charge transfer between radical ions like (TCNQ)^{•−}. In effect, the CT band in the absorption spectra of TCNQ simple salts is always very broad without any vibrational structure. Tanaka *et al.*⁵⁾ pointed out that the band B must have the character where the charge transfer between (TCNQ)^{•−} ions is mixed with the LE associated with the lowest transition of (TCNQ)^{•−}.

Recently, it was attempted by Hubbard⁸⁾ and by Kamaras *et al.*⁹⁾ to interpret the absorption spectra of TCNQ complex salts by the superposition of the spectra of (TCNQ)⁰, (TCNQ)^{•−}, and (TCNQ)₂^{•−}. However, the model adopted in these studies is too much artificial in the respect that the interactions of the three species are completely neglected.

The spectroscopic data reported so far on TCNQ

complex salts are either those obtained with powder samples or those measured on single crystals at room temperature with a relatively low resolution, so that they are not satisfactory in many respects. Thus it is most important to obtain more detailed and reliable spectroscopic data for the purpose to establish the interpretation of the visible and near-infrared spectra of TCNQ complex salts.

We have developed an experimental technique to measure the visible and near-infrared reflection spectrum of a small single crystal at temperatures in the range of 30–300 K by means of a microspectrophotometric method. We have successfully applied this technique to study the low-temperature spectrum of K(TCNQ).¹¹⁾

In the present paper, we will report the reflection spectra obtained by this method on the *N*-ethyl-1,10-phenanthroline (NEP) salt and the methyltriphenylphosphonium (MTPP) salt of TCNQ, which can be expressed as (NEP)(TCNQ)₂ and (MTPP)(TCNQ)₂, respectively. We have chosen (NEP)(TCNQ)₂ as an example of the TCNQ complex salts with a dimeric TCNQ arrangement, and (MTPP)(TCNQ)₂ as an example of the salts with a tetrameric TCNQ arrangement. We will also report the results obtained on Cs₂(TCNQ)₃.

By using these experimental data, we propose a new interpretation for the electronic spectra of TCNQ complex salts.

Experimental

The crystals of (NEP)(TCNQ)₂ were prepared from the reaction of (NEP)I and TCNQ in the acetonitrile solution. The crystals of (MTPP)(TCNQ)₂ and Cs₂(TCNQ)₃ were obtained by the method reported by Melby *et al.*¹⁰⁾ The single crystals of these salts were grown by slowly cooling the acetonitrile solution of each salt.

The visible and near-infrared reflection spectra of the small single crystals were measured at temperatures in the range of 27–300 K by using a microspectrophotometer for reflection spectroscopy combined with a cryostat to keep the sample crystal at low temperatures. The details of this apparatus have been described elsewhere.^{12,13)} The crystal faces on which the measurement of reflection spectrum was

carried out, were directly determined by X-ray diffraction using the methods of Wilsberg and/or precession photographs.

In order to obtain the absorption spectrum from the observed reflection spectrum, we used the dispersion analysis method (the curve-fitting method) by using Helmholtz-Kettler type dispersion functions. The details of this analysis method were described in our previous paper.¹²⁾

Results and Discussion

(NEP)(TCNQ)₂. The crystal of (NEP)(TCNQ)₂ is triclinic with the space group $P\bar{1}$, the lattice constants being $a=7.070$ Å, $b=14.993$ Å, $c=8.006$ Å, $\alpha=84.3^\circ$, $\beta=111.9^\circ$, and $\gamma=99.8^\circ$.¹⁴⁾ The unit cell contains one molecular unit of (NEP)(TCNQ)₂. The arrangement of TCNQ molecules (or ions) in this crystal is illustrated in Fig. 1. The infinite zigzag chain of TCNQ along the a -axis can be considered to be composed of TCNQ dimers, each of which consists of a pair of crystallographically equivalent TCNQ molecules, having one excess electron delocalized over them. We will express this dimer as (TCNQ)₂⁻. The average intermolecular separation within the dimer is 3.17 Å, which is appreciably smaller than the average intermolecular separation between the dimers, 3.46 Å.

Figure 2 shows the polarized reflection spectra measured at room temperature on the well-developed

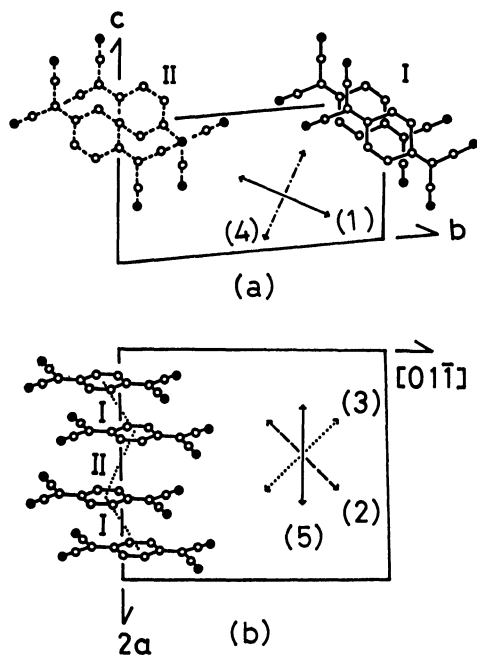


Fig. 1. (a) Projection of the TCNQ molecules onto the (100) plane in the crystal of (NEP)(TCNQ)₂. TCNQ molecules drawn by solid line shows the relative orientation of TCNQ molecules in the (TCNQ)₂⁻ dimer, TCNQ molecules drawn by dashed line shows the relative orientation of TCNQ molecules between the (TCNQ)₂⁻ dimer. (b) Projection of the TCNQ molecules onto the (011) plane. The arrows means the directions of the polarization of incident light used to measure the reflection spectra shown in Fig. 2.

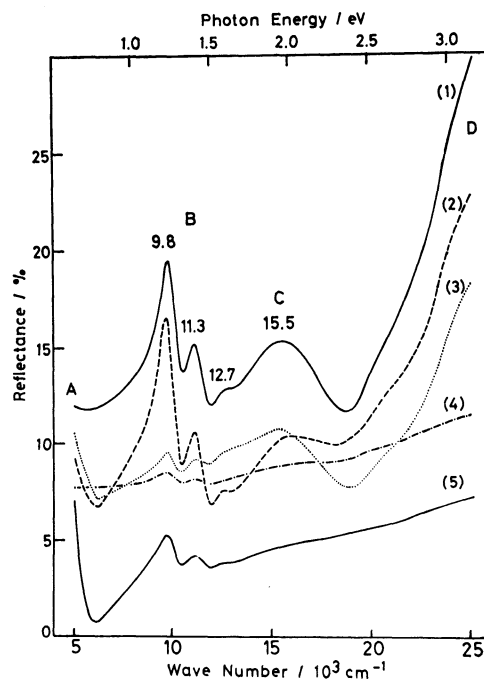


Fig. 2. Reflection spectra on the (100) and (011) crystal faces of (NEP)(TCNQ)₂. The number of each spectrum corresponds to that drawn in Figs. 1 (a) and 1 (b).

(100) and (011) crystal faces. Since (NEP)⁺ ion has no allowed electronic transition in the observed spectral range, the dispersions observed here are entirely due to the transitions associated with the TCNQ columns. The spectra show that there exist four dispersions in the observed spectral range: The first is located below 5×10^3 cm⁻¹, the second which has a sharp structure, is at about 10×10^3 cm⁻¹, the third at about 16×10^3 cm⁻¹ and the fourth above 25×10^3 cm⁻¹. These dispersions must correspond to the four absorption bands which have been reported to be characteristic of the absorption spectra of semiconductive TCNQ complex salts. Thus we will denote them as A, B, C, and D, respectively, as indicated in Fig. 2.

The polarization directions employed to measure these spectra are indicated with arrows in Fig. 1. The number given for each spectrum refers the number of the polarization direction with which the spectrum was obtained. The variation of the amplitude of a dispersion with the change of polarization direction reflects the direction of the transition moment of the electronic transition concerned. Thus one can conclude from the spectra shown in Fig. 2 that the electronic transition concerned with the dispersion A is strongly polarized in the direction of TCNQ column, while the transition concerned with the dispersion D is polarized parallel to the long molecular axis of TCNQ. According to the widely accepted interpretation of the absorption spectra of TCNQ complex salt, the dispersion A is due to the charge transfer form (TCNQ)⁻ to (TCNQ)⁰ which we will express as CT1(A→N), and the dispersion D is due to the lowest π - π^* transition of (TCNQ)⁰ which we will express as LE1(N). The observed polarizations

of these two dispersions are consistent with the assignments mentioned above.

As we have mentioned before, the band B (at about $10 \times 10^3 \text{ cm}^{-1}$) in the spectra of TCNQ complex salts has been assigned to the charge transfer between $(\text{TCNQ})^-$ ions.⁶⁾ But the corresponding dispersion (the dispersion B) clearly exhibits a sharp structure in the reflection spectra observed in the present study. We note also that the dispersion B is polarized not in the direction of the TCNQ stacking axis. To know the polarization direction that gives the maximum dispersion amplitude, we observed the variation of the amplitude by rotating the polarization direction within (011) plane. We took the difference between the reflectance values at $9.8 \times 10^3 \text{ cm}^{-1}$ (maximum) and $10.5 \times 10^3 \text{ cm}^{-1}$ (minimum), $R(9800) - R(10500)$, as the measure of the amplitude around the first peak, and the difference between the reflectance values at $11.1 \times 10^3 \text{ cm}^{-1}$ (maximum) and $11.9 \times 10^3 \text{ cm}^{-1}$ (minimum), $R(11100) - R(11900)$, as that around the second peak. The result is shown in Fig. 3, where the observed amplitudes are plotted against the angle of polarization direction θ measured from the direction of the a-axis. We can see that the θ dependence of amplitude is exactly the same between the two peaks of the dispersion B, showing a maximum at $\theta \approx 60^\circ$ which is the direction bisecting the angle between the direction of the long molecular axis of TCNQ and that connecting the centers of two TCNQ molecules within the dimer. The fact that the amplitudes of the two peaks exhibit the same angular dependence implies that they are associated with the same electronic transition.

The reflection spectra which were measured at 27 and 298 K on the (100) crystal face for the polarization (1), are shown in Fig. 4. The structure in the region of the dispersion B becomes markedly sharper at 27 K as compared with the spectrum at 298 K, while the

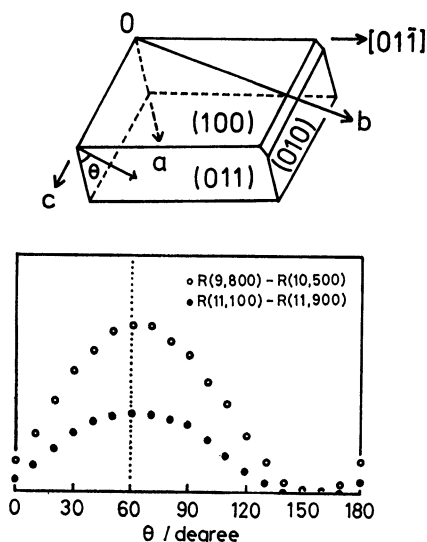


Fig. 3. The crystal shape of $(\text{NEP})(\text{TCNQ})_2$ single crystal used in this study and the angular dependency of the difference of the reflectivity between the crystal axis and polarization direction of incident light. $R(9,800)$ means the reflectivity at $9.8 \times 10^3 \text{ cm}^{-1}$.

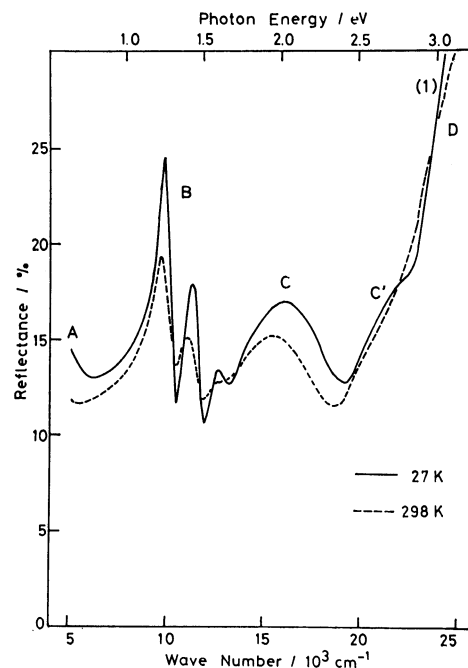


Fig. 4. Low temperature reflection spectrum polarized to the $[01\bar{1}]$ direction on the (100) face of $(\text{NEP})(\text{TCNQ})_2$. Room temperature reflection spectrum is drawn by dashed line for the purpose of comparison.

dispersion C remains broad and structureless even at 27 K. In order to see more details of the structure of the dispersion B, we carefully measured at 27 K the reflection spectrum of the concerned region with the resolution of 40 cm^{-1} . The reflectance data thus obtained are shown by points in Fig. 5 where the solid line is the best-fitted curve obtained in the final stage of the curve fitting procedure employing seven Helmholtz-Kettler oscillator functions for the region from $5 \times 10^3 \text{ cm}^{-1}$ to $25 \times 10^3 \text{ cm}^{-1}$, three oscillator functions being used for the region of the dispersion B.

In Fig. 6, the broken line shows the imaginary part of the complex dielectric function obtained by the curve

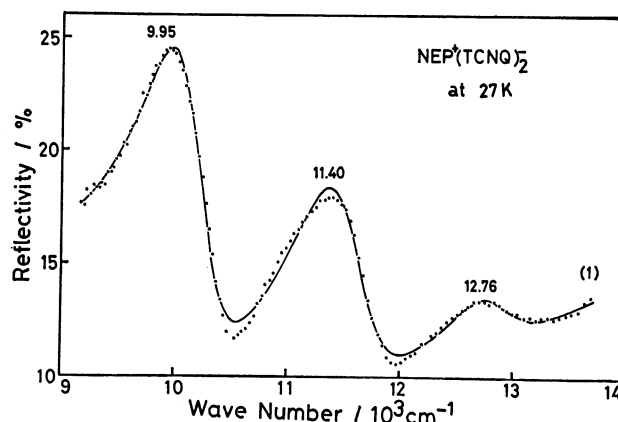


Fig. 5. The low-temperature reflection spectrum of $(\text{NEP})(\text{TCNQ})_2$ single crystal in the range from $9 \times 10^3 \text{ cm}^{-1}$ to $14 \times 10^3 \text{ cm}^{-1}$. The dots means the experimental data and the solid line is the best-fitted curve obtained by the Helmholtz-Kettler model functions.

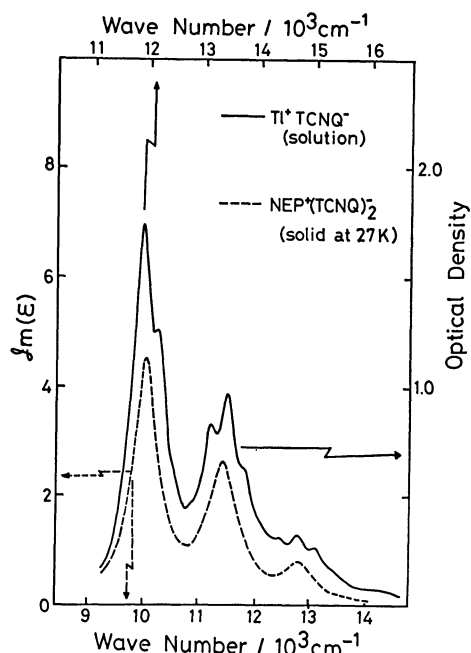


Fig. 6. Comparison between the absorption spectrum of TCNQ^- in acetonitrile solution and the imaginary part of the complex dielectric function obtained by the dispersion analysis of the reflection spectrum at low temperature.

fitting mentioned above, and the solid line is the lowest π - π^* band of $(\text{TCNQ})^-$ ion in the absorption spectrum of the acetonitrile solution of $\text{Ti}(\text{TCNQ})$. The both spectra agree quite well with each other. Such a good agreement can be expected only when the dispersion B is mainly due to the lowest π - π^* transition of $(\text{TCNQ})^-$ ion. Thus we assign the dispersion B to LE1(A) not to the charge transfer between $(\text{TCNQ})^-$ ions. Naturally, there must be a mixing with other excited configurations, in particular with CT configurations such as $\text{CT1}(\text{A} \rightarrow \text{N})$ as it is suggested from the observed polarization direction of the dispersion B.

Other interesting aspects which we note in the low-temperature spectrum, is a blue shift of the dispersion C and the appearance of a shoulder at about $22 \times 10^3 \text{ cm}^{-1}$ which we have denoted as C' in Fig. 4. The dispersion C is polarized parallel to the long molecular axis of TCNQ . As we have mentioned before, the corresponding absorption band in the absorption spectra of TCNQ complex salts has been considered to be attributable to LE1(A). We can not accept this assignment since we have already shown that it is the dispersion B that should be attributed to LE1(A). Therefore, we have to find out a new interpretation for the dispersion C.

In the ground state of $(\text{TCNQ})^0$, sixteen π electrons are occupying up to the 8th π orbital from the lowest one, and the lowest allowed π - π^* transition which gives a strong absorption band at $24.9 \times 10^3 \text{ cm}^{-1}$ in the absorption spectrum of the chloroform solution of TCNQ ,¹⁵ is associated with the transition to the singlet excited state which can be mainly expressed by the configuration where an electron has been excited from the 8th MO to the 9th MO. There must be a

triplet excited state corresponding to the singlet excited state mentioned above. This lowest triplet excited state of $(\text{TCNQ})^0$ was determined to be located at $2.0 \pm 0.2 \text{ eV}$ ($16 \times 10^3 \text{ cm}^{-1}$) above the ground state by the electron energy loss experiment.¹⁶ In the ground state of $(\text{TCNQ})^-$, π electrons are doubly occupying up to the 8th MO and singly occupying the 9th MO. The lowest π - π^* transition is associated with the excitation of an electron from the 8th MO to the 9th MO.

Let us consider the situation in the dimer $(\text{TCNQ})_2^-$, since the structural characteristics of $(\text{NEP})(\text{TCNQ})_2$ suggest that the intermolecular CT interaction is very much stronger within the dimer than between the dimers, so that the essential features of the observed reflection spectrum are expected to be understandable from the considerations on the electronic states of the dimer. The lowest CT configuration of the dimer must be the one where an electron has been transferred from the 9th MO of $(\text{TCNQ})^-$ to the 9th MO of $(\text{TCNQ})^0$. However this is not a proper expression of the CT excited state of the dimer which is composed of a pair of strictly equivalent molecules. The ground electronic configuration of such a dimer must be expressed by the two doublet configurations which are mutually different as regards the molecular site which has one unpaired electron on its 9th MO. By taking up only the 8th and 9th MO's of the two molecules, we can schematically represent the configuration as follows;

$$\left(\begin{array}{cc} \uparrow & \uparrow \\ \uparrow\downarrow & \uparrow\downarrow \end{array} \right) \pm \left(\begin{array}{cc} \uparrow & \uparrow \\ \uparrow\downarrow & \uparrow\downarrow \end{array} \right) \quad (1)$$

where the plus sign gives the gerade state and the minus sign gives the ungerade state. The gerade state must be energetically lower than the ungerade state, hence the former corresponds to the ground state of the dimer and the latter corresponds to the CT excited state. The lowest CT transition $\text{CT1}(\text{A} \rightarrow \text{N})$ is to be considered as the transition between these two states. We will attribute the dispersion A of $(\text{NEP})(\text{TCNQ})_2$ to this CT transition.

Next we will consider the charge transfer from the 8th MO of $(\text{TCNQ})^-$ to the 9th MO of $(\text{TCNQ})^0$, which can be expressed as $\text{CT2}(\text{A} \rightarrow \text{N})$. When the total spin of the dimer is considered, there will be doublet and quartet states. Since the optical transition from the ground state (doublet) is possible only to the doublet excited states, we will take up here only the doublet states. The wave function of these state can be schematically represented as follows;

$$\left(\begin{array}{cc} \uparrow & \uparrow \\ \uparrow\downarrow & \uparrow\downarrow \end{array} \right) \pm \left(\begin{array}{cc} \uparrow & \uparrow \\ \uparrow\downarrow & \uparrow\downarrow \end{array} \right) \quad (2)$$

and

$$\left(\begin{array}{cc} \uparrow & \uparrow \\ \uparrow\downarrow & \uparrow\downarrow \end{array} \right) \pm \left(\begin{array}{cc} \uparrow & \uparrow \\ \uparrow\downarrow & \uparrow\downarrow \end{array} \right) \quad (3)$$

The configurations represented by Eqs. 2 and 3 can mix with each other and also with the configurations expressed by Eq. 1 since all of them are doublet states of the dimer. When we look at the electronic configurations 2 and 3 from another side, we note that they are equivalent to the expressions of the following LE configurations of the dimer: The expression given by Eq. 2 corresponds to the state where $(\text{TCNQ})^0$ is in

the lowest singlet excited state, and $(\text{TCNQ})^-$ is in the ground state, and the expression given by Eq. 3 correspond to the state where $(\text{TCNQ})^0$ is in the lowest triplet excited state and $(\text{TCNQ})^-$ is in the ground state. Thus one could denote these configurations as $\text{LE1}(\text{N}, \text{singlet})$ and $\text{LE1}(\text{N}, \text{triplet})$ states of the dimer, respectively. It should be noted that both of them are, in reality, the doublet excited states of the dimer and, therefore, they can mix with each other as we have already mentioned (Refer the appendix for the theoretical background of the explanation mentioned here).

From these considerations, we can conclude that there will be two kinds of doublet-doublet transition associated with $\text{CT2}(\text{A} \rightarrow \text{N})$, one of which has the character of $\text{LE1}(\text{N}, \text{triplet})$ and the other has the character of $\text{LE1}(\text{N}, \text{singlet})$, and that the former transition will gain its intensity by borrowing intensity from the latter which is expected to be very strong, provided that an intermolecular CT interaction is strongly taking place in the dimer.

The doublet-doublet transition which has the character of $\text{LE1}(\text{N}, \text{triplet})$ is expected to appear at the wave number approximately equal to the energy of the lowest triplet state of TCNQ^0 ($16 \times 10^3 \text{ cm}^{-1}$).¹⁶⁾ The position of the dispersion C of $(\text{NEP})(\text{TCNQ})_2$ is in good agreement with this value. Thus, we attribute the dispersion C to the transition mentioned above, and will denote it as $\text{LE1}(\text{N}, \text{triplet})[\text{CT2}(\text{A} \rightarrow \text{N})]$. There must be a strong dispersion associated with $\text{LE1}(\text{N}, \text{singlet})[\text{CT2}(\text{A} \rightarrow \text{N})]$. We can safely assign the dispersion D to this transition.

The low-temperature spectrum of $(\text{NEP})(\text{TCNQ})_2$ exhibits a shoulder at $22 \times 10^3 \text{ cm}^{-1}$. This shoulder is

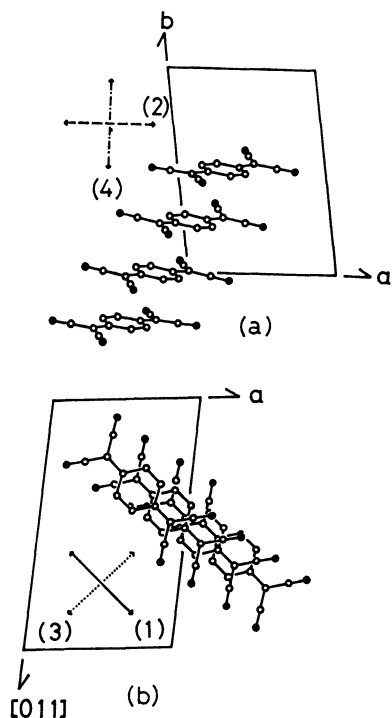


Fig. 7. Projection of the TCNQ molecules onto (a) the (001) and (b) the (011) plane in the crystal of $(\text{MTPP})(\text{TCNQ})_2$.

separated by $(11-12) \times 10^3 \text{ cm}^{-1}$ from the dispersion B which we have attributed to $\text{LE1}(\text{A})$ transition. This separation agrees with the separation between the first and second $\pi-\pi^*$ transitions of $(\text{TCNQ})^-$.¹⁷⁾ Thus we attribute the shoulder to the dispersion mainly associated with $\text{LE2}(\text{A})$.

$(\text{MTPP})(\text{TCNQ})_2$. The crystal of $(\text{MTPP})(\text{TCNQ})_2$ is triclinic with the space group PI , the lattice constants being $a=9.01 \text{ \AA}$, $b=12.89 \text{ \AA}$, $c=18.18 \text{ \AA}$, $\alpha=121.80^\circ$, $\beta=90.58^\circ$ and $\gamma=97.30^\circ$.¹⁸⁾ The unit cell contains one molecular unit of $(\text{MTPP})(\text{TCNQ})_2$. In this crystal TCNQ molecules (or ions) are forming tetramers, and a zigzag TCNQ column is formed by the stacking of these tetramers along the b-axis. The molecular arrangement within a tetramer is shown in Fig. 7. This salt exhibits a phase transition at 315 K between the low-temperature (low spin) phase and the high-temperature (high-spin) phase.¹⁹⁾ According to the results of crystal structure analysis, the molecular arrangement within the TCNQ tetramer remains the same between the two phases, but the separation of TCNQ molecules between tetramers changes from 3.57 \AA in the low-temperature phase to 3.55 \AA in the high-temperature phase.²⁰⁾ As compared with the intermolecular separation between tetramers, the molecular separations within a tetramer are appreciably small, which are reported to be 3.24, 3.22, and 3.26 \AA . Thus the main feature of the spectrum will be determined by the intermolecular interaction within the tetramer.

The absorption spectrum of the single crystal of $(\text{MTPP})(\text{TCNQ})_2$ was observed by Tanaka *et al.*,⁵⁾ and the reflection spectrum was observed by Oohashi and Sakata,⁴⁾ both the groups made the measurements only on the (001) crystal face at room temperature. These authors reported that $(\text{MTPP})(\text{TCNQ})_2$ exhibits the four absorption bands which are characteristic of the absorption spectra of TCNQ complex salts.

In the present study, we measured the reflection spectrum of this salts not only on the (001) crystal face, but also on the (011) crystal face. The polarization directions employed in those measurements are shown in Fig. 7.

Figure 8 shows the reflection spectra obtained at room temperature. From the comparison of these spectra, we can see that the dispersions denoted as B, C and D are polarized almost in the direction of the long molecular axis of TCNQ, while the dispersion A is polarized in the direction of the TCNQ column. The general features of these spectra are quite similar to the reflection spectrum of $(\text{NEP})(\text{TCNQ})_2$, except that the vibrational structure of the dispersion B less sharply appears in the spectra of $(\text{MTPP})(\text{TCNQ})_2$ than in the spectra of $(\text{NEP})(\text{TCNQ})_2$.

However, as we cool down $(\text{MTPP})(\text{TCNQ})_2$, there appears a new dispersion at about $8 \times 10^3 \text{ cm}^{-1}$, while no corresponding dispersion was found in the case of $(\text{NEP})(\text{TCNQ})_2$. We will denote this new dispersion as A' (see Fig. 9). It should be noted also that the dispersion B is blue shifted on lowering the temperature while such an appreciable temperature-dependent shift was not found in the case of $(\text{NEP})(\text{TCNQ})_2$. In other respects, the temperature dependence of the reflection

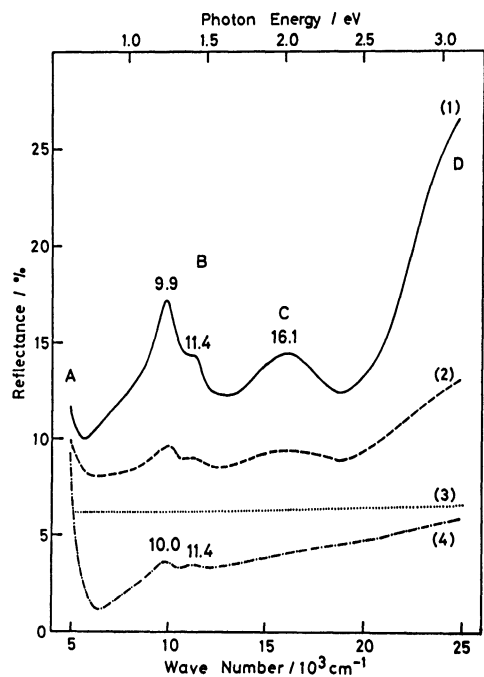


Fig. 8. Reflection spectra on the (100) and the (011) crystal faces of (MTPP)(TCNQ)₂. The number of each spectrum corresponds to that drawn in Figs. 7 (a) and 7(b).

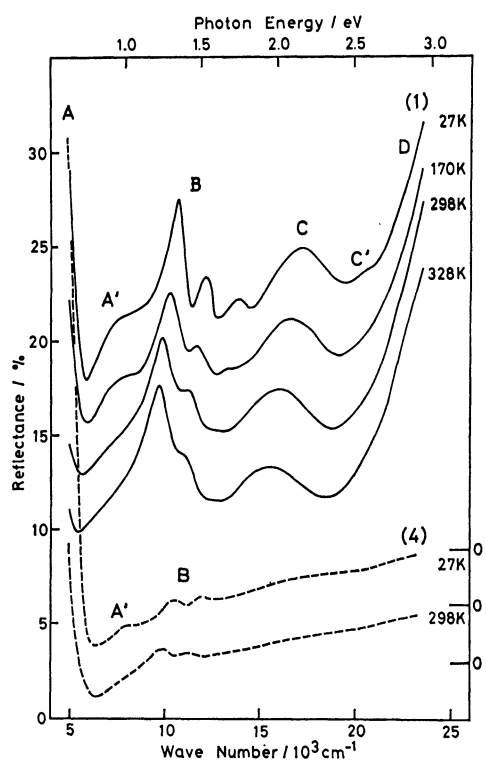


Fig. 9. Temperature dependency of the reflection spectra of (MTPP)(TCNQ)₂ single crystal polarized parallel to the [111] direction (solid line) and perpendicular to the a-axis (dashed line).

spectrum of (MTPP)(TCNQ)₂ very resembles that of (NEP)(TCNQ)₂.

The experimental results described above can be interpreted if we assume a model that the TCNQ

tetramer in (MTPP)(TCNQ)₂ is essentially composed of two TCNQ dimers, between which a CT interaction can take place. According to this model, the electronic transitions of the TCNQ tetramer can be classified into those mainly associated with the electronic transitions within each dimer and those associated with the charge transfer between the dimers. Let us consider the temperature dependence of the latter transition. Since each dimer (TCNQ)₂⁻ has one unpaired electron, there will be singlet and triplet state for the ground electronic configuration of the tetramer when the spin state is taken into account. On the other hand, the CT configuration where an electron is transferred from a singly occupied orbital of a dimer to the corresponding orbital of another dimer, is necessarily a singlet state. Consequently, the singlet ground configuration can be stabilized by the mixing with this CT configuration, but not in the case of the triplet ground configuration. The optical transition to the CT singlet state is allowed only from the singlet ground state, so that the intensity of the CT band associated with this transition should increase on lowering the temperature accompanying the increase of the population of the tetramers which are in the singlet ground state. This situation is analogous to the singlet-triplet model proposed for a radical ion dimer.

The ESR signal due to the triplet exciton in (MTPP)(TCNQ)₂ was actually observed by Chesnut and Phillip.¹⁹⁾ The temperature dependence of the paramagnetic susceptibility of this salt was approximately

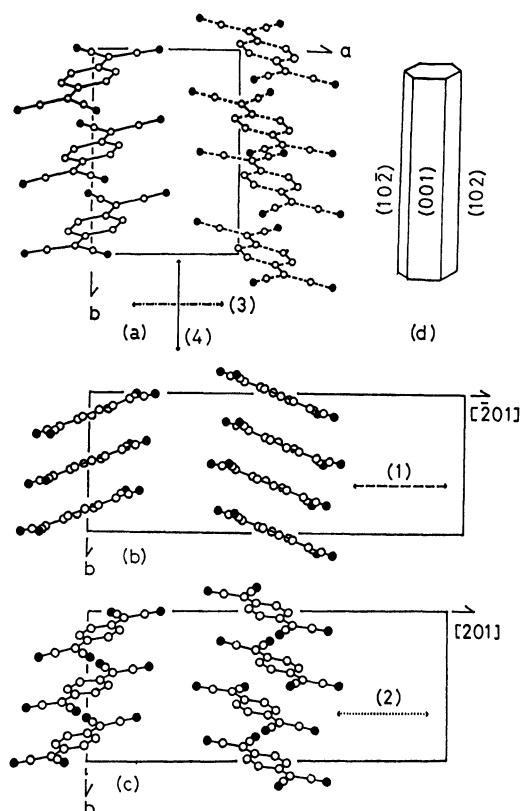


Fig. 10. Projection of the TCNQ molecules onto the crystal faces of (a) (001), (b) (102), and (c) (102). (d) Crystal morphology for Cs₂TCNQ₃ single crystal.

explained in terms of the singlet-triplet model with the energy separation of 0.065 eV.²¹⁾ This singlet-triplet separation is significantly smaller than the value (0.2–0.4 eV) usually obtained for TCNQ simple salts.²²⁾ This is also understandable from the model described above, since the stabilization of the singlet ground state caused by the CT interaction between dimers must be much smaller than that caused by the CT interaction between closely contacting (TCNQ)^{•-} ions within a (TCNQ)⁻ dimer.

According to the consideration mentioned above, we will attribute the dispersion A' which exhibits a marked increase of amplitude at lower temperature, to the charge transfer between dimers, and the remaining dispersions, A, B, C, C', and D, to the transitions within a dimer, thus attributable to the transitions which we have discussed in the cases of the corresponding dispersions of the spectrum of (NEP)(TCNQ)₂.

Cs₂(TCNQ)₃. The crystal of Cs₂(TCNQ)₃ is monoclinic with the space group P2₁/c, the lattice constants being *a*=7.34 Å, *b*=10.40 Å, *c*=21.98 Å and β=97.18°.²³⁾ The unit cell contains two molecular units of Cs₂(TCNQ)₃. The observed molecular geometries of TCNQ in this crystal indicate that the charges in the TCNQ column are rather localized, so that (TCNQ)⁰ sites and (TCNQ)^{•-} sites are regularly arranged along the column by the repetition of (TCNQ)^{•-}(TCNQ)⁰(TCNQ)^{•-} (see Fig. 10). But we should not consider that the TCNQ column is composed of discrete TCNQ trimers since the intermolecular separation is 3.22 Å between (TCNQ)⁰ and (TCNQ)^{•-} within a trimeric repeating unit and 3.26 Å between (TCNQ)^{•-} ions of the neighboring units.

Cs₂(TCNQ)₃ crystallizes as a needle-like crystal, the shape of which is illustrated in Fig. 10(d). The //b and ⊥b absorption spectra were previously observed in our laboratory on the (001) face of a single crystal at room temperature, by using a microspectrophotometer for transmission method.²⁾ The absorption spectra obtained by a similar measurement were reported later by Tanaka *et al.*⁵⁾ These two results showed a good agreement with each other. However, no observation of absorption spectrum has been done so far on the crystal faces other than the (001) face. This left some ambiguities as regards interpretation of the spectrum.

Figure 11 shows the reflection spectra measured on the (001), (102), and (10 $\bar{2}$) faces of a single crystal of Cs₂(TCNQ)₃ at room temperature. The polarization directions employed to obtain these spectra are illustrated in Fig. 10 which shows the projection of the crystal structure onto each crystal face, Cs ions having been omitted in the projections shown there. The number of each spectrum corresponds to the number of the polarization direction by which it was measured.

The spectra (3) and (4) correspond quite well to the reported absorption spectra measured on the same crystal face, (001), with the ⊥b and //b polarizations, respectively.^{2,6)} However, the spectra (1) and (2) reveal the features which have never been found from the measurements on the (001) face only. First, the spectrum (1) shows a strong maximum at 11.3×10³ cm⁻¹, which is clearly different from the position of

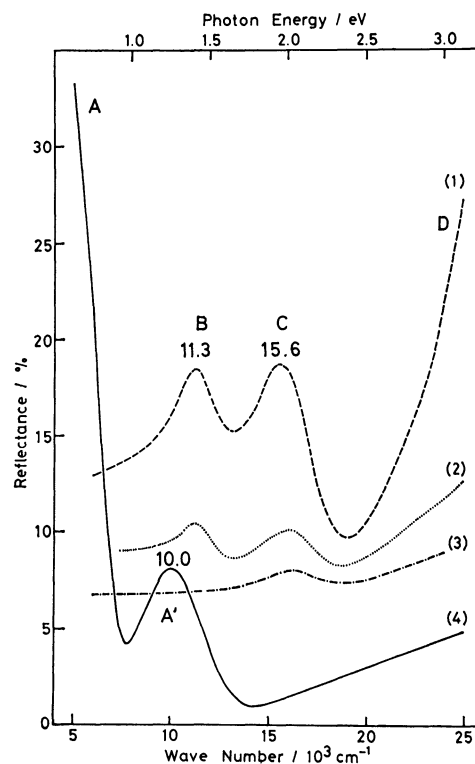


Fig. 11. Reflection spectra on the (001), the (102) and the (10 $\bar{2}$) crystal faces of Cs₂TCNQ₃ single crystal. The number of each spectrum corresponds to that drawn in Figs. 10(a), 10(b), and 10(c). The //b spectra measured on the (102) and (10 $\bar{2}$) faces were exactly the same as the //b spectrum measured on the (001) face, hence they are not shown here.

the maximum found in the spectrum (1). Second, the maximum at 15.6×10³ cm⁻¹ strongly appears in the spectrum (1) as compared with the spectra obtained with other polarizations, indicating that it is associated with the transition polarized in the direction of the long molecular axis of TCNQ.

The reflection spectra obtained at 27 K for the polarization directions (1) and (4) are shown in Fig. 12, where the broken lines are the corresponding room-temperature spectra. Note that the peak at 11.4×10³ cm⁻¹ becomes sharp and a new small peak does appear at 12.8×10³ cm⁻¹ in the spectrum (1) measured at 27 K. On the other hand, the spectrum (4) at 27 K shows a broad maximum at 10.2×10³ cm⁻¹ which is accompanied by small sharp peaks at 11.6×10³ and 13.0×10³ cm⁻¹. Probably the small sharp peaks observed in the spectrum (4) at 27 K are corresponding to the 11.4×10³ and 12.8×10³ cm⁻¹ peaks of the spectrum (1). This fact implies that the broad maximum (at 10.2×10³ cm⁻¹) of the spectrum (4) is of an origin entirely different from that of the sharp peaks which strongly appear in the spectrum (1). We note that the spectrum (1) at 27 K closely resembles the spectrum of (NEP)(TCNQ)₂, although the TCNQ column of Cs₂(TCNQ)₃ has not any discrete dimeric unit corresponding to the dimer (TCNQ)₂^{•-} which has been discussed in the case of (NEP)(TCNQ)₂. Seemingly the similarity between the

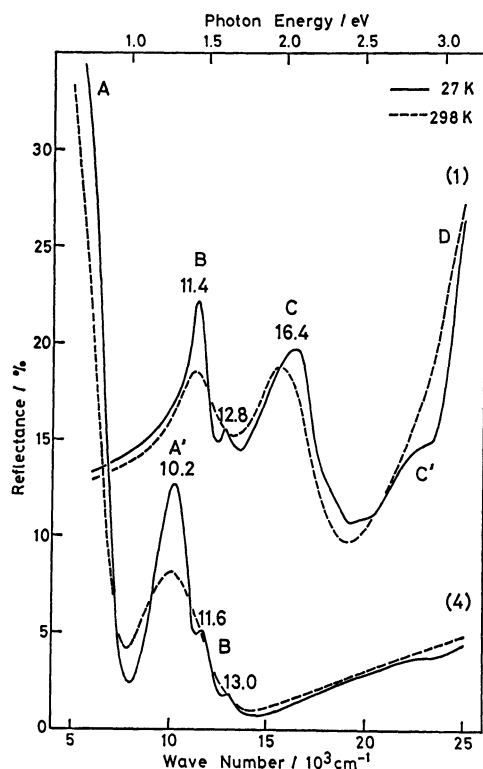


Fig. 12. Low-temperature reflection spectra of $\text{Cs}_2(\text{TCNQ})_3$ single crystal polarized parallel to the $[201]$ and the $[010]$ directions.

spectrum of $\text{Cs}_2(\text{TCNQ})_3$ and that of $(\text{NEP})(\text{TCNQ})_2$ arises because the main feature of the former is also determined by the interaction between $(\text{TCNQ})^0$ and $(\text{TCNQ})^-$. Thus, from the analogy with the assignments given for the dispersions of the spectrum of $(\text{NEP})(\text{TCNQ})_2$, we assign the dispersion B with a relatively sharp peaks at 11.4×10^3 and $12.8 \times 10^3 \text{ cm}^{-1}$ to LE1(A) and the dispersion C' which appear as a shoulder at the low-temperature spectrum (1) to LE2(A) , and the dispersion C at $16.4 \times 10^3 \text{ cm}^{-1}$ to the transition associated with the charge transfer from the second highest occupied orbital (8th MO) of TCNQ^- to the lowest unoccupied orbital (9th MO) of TCNQ^0 , thus to $\text{CT2(A} \rightarrow \text{N)}$. This $\text{CT2(A} \rightarrow \text{N)}$ transition must have a character of LE1(N, triplet) as we have pointed out in the case of $(\text{NEP})(\text{TCNQ})_2$. As a matter of fact, the dispersion C is completely polarized in the direction of the long molecular axis of TCNQ . The strong dispersion D which is located above $25 \times 10^3 \text{ cm}^{-1}$ can be safely assigned to $\text{LE1(N, singlet)}[\text{CT2(A} \rightarrow \text{N)}]$.

The dispersion A' which appears as a maximum at $10.2 \times 10^3 \text{ cm}^{-1}$ in the spectrum (4), can be assigned to the charge transfer between $(\text{TCNQ})^-$ ions, $\text{CT1(A} \rightarrow \text{A)}$. In the case of TCNQ simple salts, there exists a strong mixing between $\text{CT1(A} \rightarrow \text{A)}$ and LE1(A) . This makes the absorption band associated with LE1(A) broad and structureless, and, gives at the same time an increase of the separation between $\text{CT1(A} \rightarrow \text{A)}$ band and the band which is mainly associated with LE1(A) , their separation being usually $(5-6) \times 10^3 \text{ cm}^{-1}$ in the absorption spectra of TCNQ simple salts.

In the case of $\text{Cs}_2(\text{TCNQ})_3$, the overlap of mutually interacting $(\text{TCNQ})^-$ ions is of the short-axis-shifted mode where one of the ions is shifted against the other along the short molecular axis from the position of the direct overlap. With this mode of molecular overlap, the $\text{CT1(A} \rightarrow \text{A)}$ state cannot mix with the LE1(A) state. Probably this might be the reason why the separation between the dispersion $\text{A}'(\text{CT1(A} \rightarrow \text{A)})$ and the dispersion B (LE1(A)) is small, and the latter clearly shows a vibrational structure, although there must be a strong CT interaction between $(\text{TCNQ})^-$ ions.

Conclusion and Summary

In this study, we measured the polarized reflection spectra on the single crystals of the three different types of TCNQ complex salt, $(\text{NEP})(\text{TCNQ})_2$, $(\text{MTPP})(\text{TCNQ})_2$, and $\text{Cs}_2(\text{TCNQ})_3$, not only at room temperature but also at low temperatures down to 27 K. We have revealed that the dispersion B which appears at about $(10-11) \times 10^3 \text{ cm}^{-1}$ shows a sharp structure corresponding to the vibrational structure of the lowest $\pi-\pi^*$ band of the solution spectrum of $(\text{TCNQ})^-$ ion, and is polarized in the direction rather close to the direction of the long molecular axis of TCNQ . We have also found that a new dispersion appears at $(7-8) \times 10^3 \text{ cm}^{-1}$ in the low-temperature spectrum of $(\text{MTPP})(\text{TCNQ})_2$ and its amplitude increases on lowering the temperature. The low-temperature spectrum of $\text{Cs}_2(\text{TCNQ})_3$ showed that there is a broad dispersion at $10.2 \times 10^3 \text{ cm}^{-1}$, polarized parallel to the TCNQ column, besides a sharp dispersion at $11.4 \times 10^3 \text{ cm}^{-1}$ polarized in the direction of the long-molecular axis of $(\text{TCNQ})^-$.

These new results cannot be explained by the interpretations which have been hitherto proposed for the absorption bands of the spectra of semiconductive TCNQ complex salts.

On the bases of those experimental results, we have proposed a new interpretation, particularly for the origin of the dispersion B which appears at about $10 \times 10^3 \text{ cm}^{-1}$ with a vibrational structure and the dispersion C which appears at about $16 \times 10^3 \text{ cm}^{-1}$.

Finally we wish to point out that, as we have revealed in this study, it is extremely important to observe the reflection (or absorption) spectra on various crystal faces with different polarizations, not only at room temperature but also at low temperatures in order to know the true characteristics of the spectra of highly anisotropic organic solids such as TCNQ salts, and to establish the interpretations of the spectra.

The authors wish to thank Mr. Nobuhiro Kosugi for helpful discussion.

Appendix

We will consider the ground and excited states of the dimer $(\text{TCNQ})_2^-$ by using a simple configuration interaction method, in order to reveal the mechanism of the mixing of the states of the doublet-singlet pair and the doublet-triplet pair. To simplify the model we take account only of the 8th and 9th

molecular orbitals of TCNQ. Let us express the wave functions of various configurations of the dimer as follows denoting the molecules in the dimer as A and B, respectively;

$$\begin{aligned}
 \text{(i)} \quad \Phi_{GA}^{\alpha} &= \left(\begin{array}{cc} \uparrow & \uparrow \\ \uparrow & \uparrow \end{array} \right) = |8_A \bar{8}_A 9_A 8_B \bar{8}_B| \\
 \Phi_{GB}^{\alpha} &= \left(\begin{array}{cc} \uparrow & \uparrow \\ \uparrow & \uparrow \end{array} \right) = |8_A \bar{8}_A 8_B \bar{8}_B 9_B| \\
 \text{(ii)} \quad \Phi_{DA}^{\alpha} &= \left(\begin{array}{cc} \uparrow & \uparrow \\ \uparrow & \uparrow \end{array} \right) = |8_A 9_A \bar{8}_A 8_B \bar{8}_B| \\
 \Phi_{DB}^{\alpha} &= \left(\begin{array}{cc} \uparrow & \uparrow \\ \uparrow & \uparrow \end{array} \right) = |8_A \bar{8}_A 8_B 9_B \bar{8}_B| \\
 \text{(iii)} \quad \Phi_{TA}^{\alpha} &= \\
 &= \frac{1}{\sqrt{6}} \{ 2 \left(\begin{array}{cc} \uparrow & \uparrow \\ \uparrow & \uparrow \end{array} \right) - \left(\begin{array}{cc} \uparrow & \uparrow \\ \uparrow & \uparrow \end{array} \right) - \left(\begin{array}{cc} \uparrow & \uparrow \\ \uparrow & \uparrow \end{array} \right) \} \\
 &= \frac{1}{\sqrt{6}} \{ 2 |8_A 9_A 8_B \bar{8}_B \bar{8}_B| - |8_A 9_A 8_B \bar{8}_B 9_B| \\
 &\quad - |8_A \bar{8}_A 8_B \bar{8}_B 9_B| \} \\
 \Phi_{TB}^{\alpha} &= \\
 &= \frac{1}{\sqrt{6}} \{ 2 \left(\begin{array}{cc} \uparrow & \uparrow \\ \uparrow & \uparrow \end{array} \right) - \left(\begin{array}{cc} \uparrow & \uparrow \\ \uparrow & \uparrow \end{array} \right) - \left(\begin{array}{cc} \uparrow & \uparrow \\ \uparrow & \uparrow \end{array} \right) \} \\
 &= \frac{1}{\sqrt{6}} \{ 2 |8_A \bar{8}_A \bar{8}_B 9_B| - |8_A \bar{8}_A 9_A \bar{8}_B 9_B| \\
 &\quad - |8_A \bar{8}_A 9_A 8_B \bar{8}_B| \} \\
 \text{(iv)} \quad \Phi_{SA}^{\alpha} &= \frac{1}{\sqrt{2}} \{ \left(\begin{array}{cc} \uparrow & \uparrow \\ \uparrow & \uparrow \end{array} \right) - \left(\begin{array}{cc} \uparrow & \uparrow \\ \uparrow & \uparrow \end{array} \right) \} \\
 &= \frac{1}{\sqrt{2}} \{ |8_A 9_A 8_B \bar{8}_B 9_B| - |8_A \bar{8}_A 8_B \bar{8}_B 9_B| \} \\
 \Phi_{SB}^{\alpha} &= \frac{1}{\sqrt{2}} \{ \left(\begin{array}{cc} \uparrow & \uparrow \\ \uparrow & \uparrow \end{array} \right) - \left(\begin{array}{cc} \uparrow & \uparrow \\ \uparrow & \uparrow \end{array} \right) \} \\
 &= \frac{1}{\sqrt{2}} \{ |8_A \bar{8}_A 9_A \bar{8}_B 9_B| - |8_A \bar{8}_A 9_A 8_B \bar{8}_B| \}
 \end{aligned}$$

where α represents the spin state of the doublet system, 8_A and 8_B mean the 8th molecular orbital of the molecule A with α spin and that of the molecule B with β spin, and $|8_A \bar{8}_A 9_A 8_B \bar{8}_B|$ means the Slater determinant.

When we neglect the intermolecular interaction, (i), (ii), (iii), and (iv) correspond, respectively, to the ground configuration, the LE configurations associated with the first excited state of TCNQ⁻, the ones associated with the first triplet and singlet excited states of TCNQ⁰. When the intermolecular interaction H_{AB} is introduced, the electronic states of the dimer can be described by the linear combination of these states. As the first approximation, we will take account of the following transfer integrals:

$$\begin{aligned}
 t_0 &= \langle \Phi_{GA}^{\alpha} | H | \Phi_{GB}^{\alpha} \rangle \simeq \langle |8_A 9_A \bar{8}_A 8_B \bar{8}_B| H | 8_A 9_A 8_B \bar{8}_B \bar{8}_B| \rangle \\
 &= \langle |8_A \bar{8}_A 8_B 9_B \bar{8}_B| H | 8_A \bar{8}_A \bar{8}_B 9_B \bar{8}_B| \rangle \\
 &\simeq -\langle |8_A 9_A \bar{8}_A 8_B \bar{8}_B| H | 8_A \bar{8}_A 8_B \bar{8}_B 9_B| \rangle \\
 &= -\langle |8_A \bar{8}_A 8_B 9_B \bar{8}_B| H | 8_A \bar{8}_A 9_A 8_B \bar{8}_B| \rangle \\
 t_1 &= -\langle |8_A \bar{8}_A 8_B \bar{8}_B| H | 8_A 9_A 8_B \bar{8}_B \bar{8}_B| \rangle \\
 &= -\langle |8_A \bar{8}_A 8_B \bar{8}_B 9_B| H | 8_A \bar{8}_A \bar{8}_B 9_B \bar{8}_B| \rangle \\
 &\simeq \langle |8_A \bar{8}_A 9_A \bar{8}_B 8_B| H | \bar{8}_A 9_A 8_B \bar{8}_B 9_B| \rangle \\
 &= \langle |8_A \bar{8}_A 8_B \bar{8}_B 9_B| H | 8_A \bar{8}_A 9_A \bar{8}_B 9_B| \rangle \\
 t_2 &= \langle |8_A 9_A 8_B \bar{8}_B \bar{8}_B| H | 8_A \bar{8}_A 9_A 8_B \bar{8}_B| \rangle \\
 &= \langle |8_A \bar{8}_A 8_B \bar{8}_B 9_B| H | 8_A \bar{8}_A \bar{8}_B 9_B \bar{8}_B| \rangle \\
 &\simeq \langle |8_A 9_A 8_B \bar{8}_B 9_B| H | 8_A \bar{8}_A 9_A \bar{8}_B 9_B| \rangle,
 \end{aligned}$$

where, $H=H_0+H_{AB}$. The origin of the energy is chosen so that $\langle \Phi_{GA}^{\alpha} | H | \Phi_{GA}^{\alpha} \rangle$ is equal to zero. The matrix of the secular equation will be given by (1) for the gerade states,

$$\begin{pmatrix} \Phi_G^+ \\ \Phi_D^+ \\ \Phi_T^+ \\ \Phi_S^+ \end{pmatrix} \begin{pmatrix} t_0 & 0 & -\frac{3}{\sqrt{6}}t_1 & \frac{1}{\sqrt{2}}t_1 \\ & E_D & \frac{3}{\sqrt{6}}t_0 & \frac{1}{\sqrt{2}}t_0 \\ & & E_T - \frac{1}{2}t_2 & -\frac{\sqrt{3}}{2}t_2 \\ & & & E_S + \frac{1}{2}t_2 \end{pmatrix} \begin{pmatrix} \Phi_G^+ \\ \Phi_D^+ \\ \Phi_T^+ \\ \Phi_S^+ \end{pmatrix} \quad (1)$$

and by (2) for the ungerade states,

$$\begin{pmatrix} \Phi_G^- \\ \Phi_D^- \\ \Phi_T^- \\ \Phi_S^- \end{pmatrix} \begin{pmatrix} -t_0 & 0 & -\frac{3}{\sqrt{6}}t_1 & \frac{1}{\sqrt{2}}t_1 \\ & E_D & \frac{3}{\sqrt{6}}t_0 & \frac{1}{\sqrt{2}}t_0 \\ & & E_T + \frac{1}{2}t_2 & \frac{\sqrt{3}}{2}t_2 \\ & & & E_S - \frac{1}{2}t_2 \end{pmatrix} \begin{pmatrix} \Phi_G^- \\ \Phi_D^- \\ \Phi_T^- \\ \Phi_S^- \end{pmatrix} \quad (2)$$

where,

$$\begin{aligned}
 \Phi_G^{\pm} &= \frac{1}{\sqrt{2}} (\Phi_{GA}^{\alpha} \pm \Phi_{GB}^{\alpha}) \\
 \Phi_D^{\pm} &= \frac{1}{\sqrt{2}} (\Phi_{DA}^{\alpha} \pm \Phi_{DB}^{\alpha}) \\
 \Phi_T^{\pm} &= \frac{1}{\sqrt{2}} (\Phi_{TA}^{\alpha} \pm \Phi_{TB}^{\alpha}) \\
 \Phi_S^{\pm} &= \frac{1}{\sqrt{2}} (\Phi_{SA}^{\alpha} \pm \Phi_{SB}^{\alpha})
 \end{aligned}$$

The integrals, t_0 , t_1 , and t_2 , have negative values because of the symmetry of the molecular orbitals²⁴⁾ and the geometrical configuration of TCNQ molecules in the dimer. Therefore, the ground state of this system will be Φ_G^+ , and the optical transition from this state is allowed only to Φ_G^- , Φ_D^- , Φ_T^- , and Φ_S^- . The wave function of the ground state and those of the ungerade states can be expressed as follows when they are calculated by the first order perturbation method.

$$\begin{aligned}
 \Phi_G &= \Phi_G^+ + \frac{\frac{3}{\sqrt{6}}t_1}{E_T - \frac{1}{2}t_2 - t_0} \Phi_T^+ - \frac{\frac{1}{\sqrt{2}}t_1}{E_S + \frac{1}{2}t_2 - t_0} \Phi_S^+ \\
 \Phi_{GT} &= \Phi_G^- + \frac{\frac{3}{\sqrt{6}}t_1}{E_T + \frac{1}{2}t_2 + t_0} \Phi_T^- - \frac{\frac{1}{\sqrt{2}}t_1}{E_S - \frac{1}{2}t_2 + t_0} \Phi_S^- \\
 \Phi_D &= \Phi_D^- - \frac{\frac{3}{\sqrt{6}}t_0}{E_T + \frac{1}{2}t_2 - E_D} \Phi_T^- - \frac{\frac{\sqrt{3}}{2}t_0}{E_S - \frac{1}{2}t_2 - E_D} \Phi_S^- \\
 \Phi_T &= \Phi_T^- - \frac{\frac{3}{\sqrt{6}}t_1}{E_T + \frac{1}{2}t_2 + E_D} \Phi_G^- + \frac{\frac{3}{\sqrt{6}}t_0}{E_T + \frac{1}{2}t_2 - E_D} \Phi_D^- \\
 &\quad - \frac{\frac{\sqrt{3}}{2}t_2}{E_S - t_2 - E_T} \Phi_S^-
 \end{aligned}$$

$$\Phi_s = \Phi_s^- + \frac{\frac{1}{\sqrt{2}}t_1}{E_s - \frac{1}{2}t_2 + t_0} \Phi_G^- + \frac{\frac{1}{\sqrt{2}}t_0}{E_s - \frac{1}{2}t_2 - E_D} \Phi_D^- \\ + \frac{\frac{\sqrt{3}}{2}t_2}{E_s - t_2 - E_T} \Phi_T^-$$

The transitions to Φ_{CT} , Φ_D , Φ_T , and Φ_s from Φ_G correspond to $CT1(A \rightarrow N)$, $LE1(A)$, $LE1(N, \text{triplet})$ and $LE1(N, \text{singlet})$, respectively, and the last two transitions have, at the same time, the nature of $CT2(A \rightarrow N)$. Thus, the transition $\Phi_G \rightarrow \Phi_T$ can borrow its intensity from the very strong transition of the type $\Phi_G^+ \rightarrow \Phi_s^-$, provided that t_2 is not zero. Although the present formulation has been carried out by taking up only the 8th and 9th MO, the conclusion will not change qualitatively even if we carried out a more elaborate calculation.

References

- 1) Y. Iida, *Bull. Chem. Soc. Jpn.*, **42**, 637 (1969).
- 2) S. Hiroma, H. Kuroda, H. Akamatu, *Bull. Chem. Soc. Jpn.*, **44**, 9 (1971).
- 3) A. Brau, P. Bruesch, J. P. Farges, W. Hinz, and D. Kuse, *Phys. Status Solidi B*, **62**, 615 (1974).
- 4) Y. Oohashi and T. Sakata, *Bull. Chem. Soc. Jpn.*, **48**, 1725 (1975).
- 5) J. Tanaka, M. Tanaka, T. Kawai, T. Tanabe, and O. Maki, *Bull. Chem. Soc. Jpn.*, **49**, 2358 (1976).
- 6) J. B. Torrance, B. A. Scott, and F. B. Kaufman, *Solid State Commun.*, **17**, 1369 (1975).
- 7) J. B. Torrance, Proc. Conf. on Organic Metals and Semiconductors, p. 453, Siófok, Hungary, Sept. 1976.
- 8) J. Hubbard; *Phys. Rev. B*, **17**, 494 (1978).
- 9) K. Kamaras, G. Gruner, and G. A. Sawatzky, *Solid State Commun.*, **27**, 1171 (1978).
- 10) L. R. Melby, R. J. Harder, W. R. Hertler, W. Mahler, R. E. Benson, and W. E. Mochel, *J. Am. Chem. Soc.*, **84**, 3374 (1962).
- 11) K. Yakushi, T. Kusaka, and H. Kuroda, *Chem. Phys. Lett.*, **68**, 139 (1979).
- 12) K. Yakushi, M. Iguchi, and H. Kuroda, *Bull. Chem. Soc. Jpn.*, **52**, 3180 (1979).
- 13) Y. Iyechika, K. Yakushi, and H. Kuroda, *Bull. Chem. Soc. Jpn.*, **53**, 603 (1980).
- 14) D. Chasseau, J. Gaultier, and C. Hauw, *Acta Crystallogr., Sect. B*, **32**, 3262 (1976).
- 15) R. R. Pennelly and C. J. Eckhardt, *Chem. Phys.*, **12**, 89 (1976).
- 16) J. J. Ritsko, L. J. Brillson, and D. J. Sandman, *Solid State Commun.*, **24**, 109 (1977).
- 17) Y. Oohashi and T. Sakata, *Bull. Chem. Soc. Jpn.*, **46**, 3330 (1973).
- 18) A. T. McPhail, G. M. Semeniuk, D. B. Chesnut, and P. M. Gross, *J. Chem. Soc., A*, **1971**, 2174.
- 19) D. B. Chesnut and W. D. Phillips, *J. Chem. Phys.*, **35**, 1002 (1961).
- 20) M. Konno and Y. Saito, *Acta Crystallogr., Sect. B*, **29**, 2815 (1973).
- 21) R. G. Kepler, *J. Chem. Phys.*, **39**, 3528 (1963).
- 22) Z. Soos, "Molecular Association," ed by R. Foster, Academic Press (1975), Vol. 1, p. 1.
- 23) C. J. Fritchie, Jr., and P. Arthur, Jr., *Acta Crystallogr.*, **21**, 139 (1966).
- 24) The symmetry of the 8th and 9th MO is b_{1u} and b_{2g} , respectively.